Rapid Communications

Current scaling of the topological quantum phase transition between a quantum anomalous Hall insulator and a trivial insulator

Minoru Kawamura,[1,*] Masataka Mogi,[2] Ryutaro Yoshimi,[1] Atsushi Tsukazaki,[3] Yusuke Kozuka,[2] Kei S. Takahashi,[1,4] Masashi Kawasaki,[1,2] and Yoshinori Tokura[1,2,5]

[1]*RIKEN Center for Emergent Matter Science (CEMS), Wako 351-0198, Japan*

[2]*Department of Applied Physics and Quantum-Phase Electronics Center (QPEC), University of Tokyo, Tokyo 113-8656, Japan*

[3]*Institute for Materials Research, Tohoku University, Sendai 980-8577, Japan*

[4]*PRESTO, Japan Science and Technology Agency (JST), Tokyo 102-0075, Japan*

[5]*Tokyo College, University of Tokyo, Tokyo 113-8656, Japan*

(Received 10 May 2020; accepted 29 June 2020; published 16 July 2020)

We report a current scaling study of a quantum phase transition between a quantum anomalous Hall insulator and a trivial insulator on the surface of a heterostructure film of magnetic topological insulators. The transition was observed by tilting the magnetization while measuring the Hall conductivity σ_{xy}. The transition curves of σ_{xy} taken under various excitation currents cross each other at a single point, exemplifying a quantum critical behavior of the transition. The slopes of the transition curves follow a power-law dependence of the excitation current, giving a scaling exponent. Combining with the result of the previous temperature scaling study, critical exponents ν for the localization length and p for the coherence length are separately evaluated as $\nu = 2.8 \pm 0.3$ and $p = 3.3 \pm 0.3$.

DOI: 10.1103/PhysRevB.102.041301

Topological phases of matter have been one of the central research topics in contemporary condensed-matter physics [1–3]. A quantum phase transition (QPT) between two topologically distinct phases can be characterized by a change in the topological index of gapped bulk energy bands even if the symmetry does not change. According to the bulk-edge correspondence, the QPT is accompanied by a closing of the energy gap at the quantum critical point (QCP), resulting in abrupt changes in physical quantities such as transport coefficients.

Quantum anomalous Hall (QAH) insulator is one of the most distinct topological phases materialized on the surface of ferromagnetic topological insulators [4–11]. Magnetic exchange interaction between itinerant surface electrons and localized magnetic moments opens an energy gap in the dispersion relation of the surface state, stabilizing the QAH insulator phase. The QAH insulator possesses a one-dimensional chiral edge channel running on the side surface of a sample which contributes to the quantized Hall conductivity of e^2/h, where e is the elementary charge and h is the Planck's constant. The QAH effect has been studied intensively in a family of magnetically doped topological insulators Cr- and/or V-doped $(Bi,Sb)_2Te_3$ and their heterostructure films. Recently, materials hosting the QAH effect have been expanded to include a stoichiometric magnetic topological insulator $MnBi_2Te_4$ [12,13] and twisted bilayer graphene [14,15]. Recent experimental studies have explored various insulator phases in magnetic topological insulators such as an axion insulator under antiparallel magnetizations [16,17], a trivial insulator stabilized by the hybridization of top and bottom surface states [18–20], and an Anderson insulator [21]. Since then, the QPTs between the QAH insulator and the other insulator phases have attracted considerable attention [12,19–22].

The QPTs between the QAH insulator and the other insulator phases are signaled by changes in the Hall conductivity σ_{xy}, which is an e^2/h multiple of the Chern number [23]. The QPTs possess many similarities to the plateau-plateau transitions of the quantum Hall (QH) effect in semiconductor two-dimensional systems [24–39]. The QH transitions are characterized by a divergence of the localization length $\xi \propto |E - E_c|^{-\nu}$ as the QCP is approached, where E_c is a critical energy and ν is a critical exponent for the localization length. Theoretical studies have shown the universal exponent $\nu = 2.6$ for a quantum network of chiral edge channels while $\nu = 4/3$ for a classical network [26–31]. Because a critical exponent of a QPT is believed to reflect only fundamental symmetries and dimensionality of a system regardless of its detailed physical realization, the critical exponent is predicted to be $\nu = 2.6$ [40] for the QPT between the QAH insulator and an axion insulator, which is the same as the result of the Chalker-Coddington model for the QH transitions [30,31]. A Berezinskii-Kosterlitz-Thouless (BKT) -type phase transition and a slightly different critical exponent $\nu = 2.4$ are also theoretically proposed when random magnetic domains are involved [41].

Experimentally, the QPTs have been studied in ferromagnetic topological insulator thin films by reversing the magnetization [20], by changing the carrier density [21], or by changing the magnetization direction [19]. The critical

*minoru@riken.jp

behaviors of the QPTs were studied by the temperature (T) scaling of the transport coefficients where the sharpness of the transition (ΔE^{-1}) scales as $\Delta E^{-1} \sim T^{-\kappa}$ with a critical exponent κ. In these studies, κ ranging from 0.22 to 0.62 are reported. However, the exponent κ is a combination value ($=p/2\nu$, as shown below) of ν and another exponent p for the coherence length ($l_\phi \sim T^{-p/2}$) [24]. To compare the experimentally observed critical exponent with the theories, an independent measurement of p is essential.

In this Rapid Communication, the two critical exponents p and ν of the QPT between the QAH insulator and the trivial insulator are separately evaluated employing a current scaling technique developed in the earlier studies of the QH transitions [36–39]. The QPT was driven by tilting the magnetization in a heterostructure film of magnetic topological insulator as similar to a previous study [19]. Because only the magnetization component perpendicular to the film plane contribute tos the exchange gap energy, the exchange gap energy can be tuned by tilting the magnetization with the assistance of external magnetic fields. The QPT occurs when the exchange gap energy meets the hybridization energy caused by the coupling of the top and bottom surface states [19,42]. In this method, all the magnetic moments are forced to align in the direction of the external field, therefore complications arising from the magnetic domain formation are avoided. We observe transitions of σ_{xy} from e^2/h to zero as the magnetization is tilted away from the direction perpendicular to the film plane. By analyzing the current dependence of the transition curves, a current scaling exponent is determined. Combining with the result of the previous temperature scaling study, the critical exponents ν and p are separately evaluated as $\nu = 2.8 \pm 0.3$ and $p = 3.3 \pm 0.3$.

In the theoretical studies [28,31], the exponent ν is evaluated numerically using the finite-size scaling method changing the system size. In the experimental studies, instead of the system size, the phase coherence length l_ϕ is changed through temperature T. In a diffusive system, the phase coherence time τ_ϕ follows a power law as $\tau_\phi \sim T^{-p}$, leading to $l_\phi \sim T^{-p/2}$. Then, by putting l_ϕ as a cutoff length, the sharpness of the transition follows a power law $\Delta E^{-1} \propto T^{-\kappa}$ with $\kappa = p/2\nu$ [24,32]. In the current scaling analysis, the mean energy drop between coherent regions is regarded as an effective temperature: $k_B T_{\rm eff} = eRI/(L/l_\phi)$, where k_B is the Boltzmann's constant, R the sample resistance, I the excitation current, and L the sample size. Then, l_ϕ is related to I as $l_\phi \propto I^{-p/(p+2)}$. Consequently, the sharpness of the transition follows a power law $\Delta E^{-1} \propto I^{-b}$ with $b = p/(p+2)\nu$. Therefore, by measuring κ and b experimentally, ν and p can be determined separately [36,37].

Experiments were conducted using a Hall-bar sample [Fig. 1(a)] identical to the previous study [19]. The Hall bar was made from a heterostructured film of $(Bi,Sb)_2Te_3$ sandwiched by 2-nm-thick Cr-doped $(Bi,Sb)_2Te_3$ grown on InP(111) substrate by molecular beam epitaxy (MBE) as schematically shown in Fig. 1(b). The total thickness of the film was 8 nm. The Bi/Sb ratio was adjusted so that the Fermi energy lies close to the charge neutrality point. Details of the sample preparation are described elsewhere [16]. Low-temperature transport measurements were conducted at $T = 100$ mK using a dilution refrigerator equipped with a single-axis sample rotator. A low-frequency lock-in technique was employed for the resistance measurement. The excitation current was applied through a resistance of 10 or 1 MΩ connected to the sample in series.

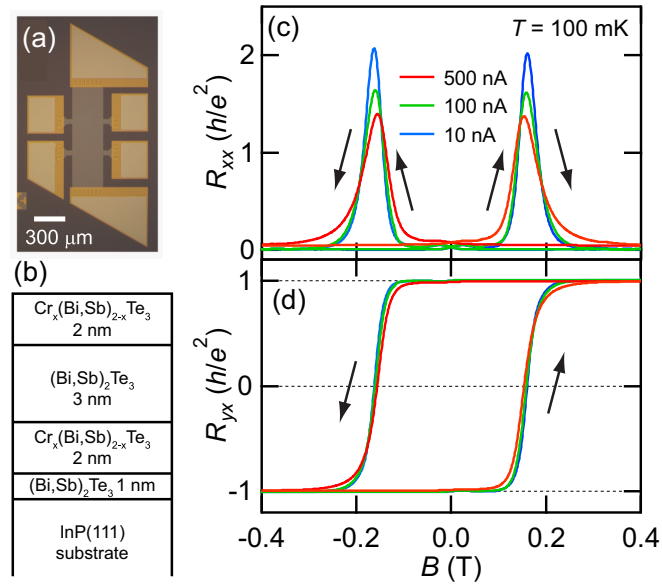

FIG. 1. (a) Photograph of the Hall bar sample. (b) Schematic structure of the magnetic topological insulator heterostructure film. The Cr content $x = 0.24$. (c)(d) Magnetic field dependence of R_{xx} (c) and R_{yx} (d) at $T = 100$ mK measured using the excitation current $I = 10$ nA, 100 nA, and 500 nA. The data were taken by sweeping the field in the positive and negative directions indicated by arrows at a rate of 0.03 T/min.

Figures 1(c) and 1(d) respectively show the magnetic field dependence of R_{xx} and R_{yx} under application of excitation current $I = 10$, 100, and 500 nA. The magnetic field was applied almost perpendicular to the film plane. The QAH effect with the quantized Hall resistance h/e^2 is clearly observed. The sign of the Hall resistance changes when the magnetization is reversed, accompanied by a peak in R_{xx}. As the excitation current is increased, the R_{xx} peaks are broadened and the slopes of the Hall resistance curves become gentle at the magnetic fields near the coercive fields. At $I = 500$ nA, R_{xx} is lifted off from zero at $B = 0.5$ T and R_{yx} is slightly decreased from h/e^2. Thus, the increase in excitation current gives qualitatively similar effects on the R_{xx}-B and R_{yx}-B curves as the increase in temperature.

Figures 2(a) and 2(b) show the current dependence of R_{xx} and R_{yx} under various magnetization angles, respectively. In this measurement, an external magnetic field $|B| = 2$ T, which is much larger than the coercive field of the present sample, was applied and was rotated to tilt the magnetization direction using the single-axis sample rotator. The tilted angle θ is measured from the direction perpendicular to the film plane. When the magnetization is almost perpendicular to the film plane ($\theta = 2.3°$), the value of R_{xx} increases steeply as I exceeds 100 nA, accompanied by a deviation of R_{yx} from h/e^2. This corresponds to the current-induced breakdown of the QAH effect [43]. When the magnetization is almost parallel to the film plane ($\theta = 89.7°$), the value of R_{xx} decreases with

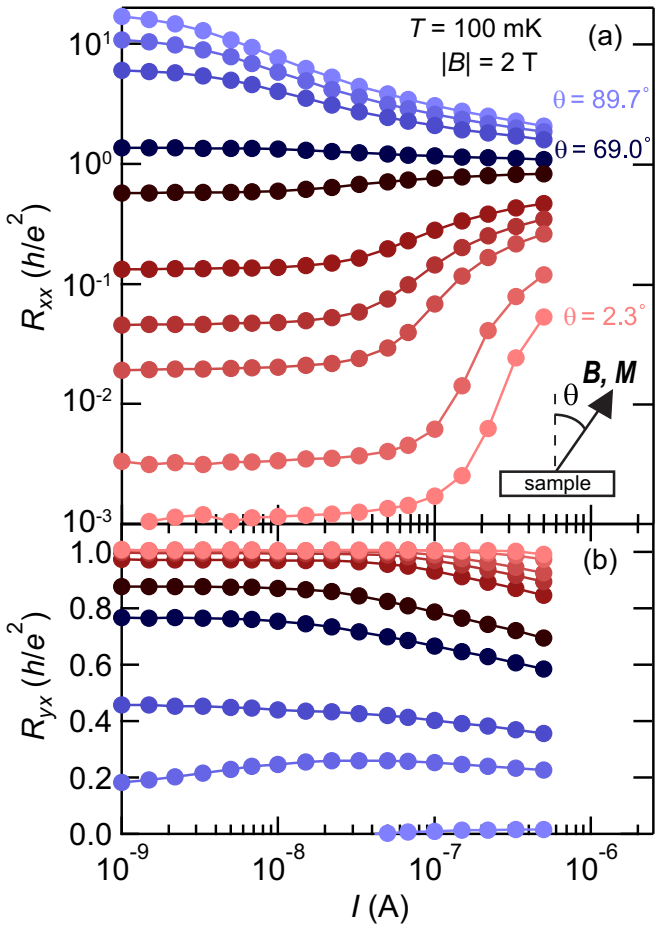

FIG. 2. (a)(b) Current dependence of R_{xx} (a) and R_{yx}(b) at $|B| = 2$ T and $T = 100$ mK under various magnetic field angles θ. Data for $\theta = 2.3°$, 28.2°, 42.7°, 47.9°, 53.2°, 63.7°, 69.0°, 78.1°, 82.5°, and 89.7° are plotted from bottom to top in (a). θ is measured from the direction perpendicular to the film as depicted in the inset in (a).

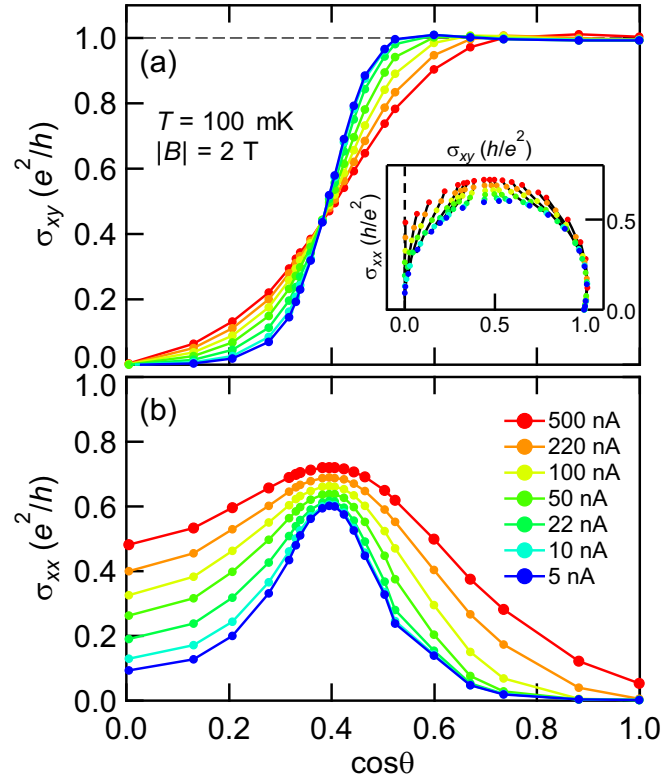

FIG. 3. (a)(b) Magnetization angle dependence of σ_{xy} (a) and σ_{xx} (b) plotted as a function of $\cos\theta$. The conductivity tensor components are converted from the resistance data shown in Fig. 2 using the relation $\sigma_{xy} = \rho_{yx}/(\rho_{xx}^2 + \rho_{yx}^2)$ and $\sigma_{xx} = \rho_{xx}/(\rho_{xx}^2 + \rho_{yx}^2)$. The data for several excitation currents ranging from 5 nA to 500 nA are shown. The inset in (a) shows a parametric plot of $(\sigma_{xy}, \sigma_{xx})$. Each black curve connects the points belonging to the same magnetization angle.

increasing the excitation current. This current dependence is a typical behavior of a trivial insulator. At the intermediate angles around $\theta = 69.0°$ where R_{xx} is close to h/e^2, R_{xx} is nearly independent of I.

To see the critical behavior of the QPT, the conductivity tensor components σ_{xx} and σ_{xy} calculated from R_{xx} and R_{yx} are plotted as a function of $\cos\theta$ in Fig. 3. The Hall conductivity σ_{xy} transits from e^2/h to zero as $\cos\theta$ is decreased [Fig. 3(a)]. The transition in σ_{xy} is accompanied by a peak in σ_{xx} [Fig. 3(b)], reflecting the energy gap closing at the QCP. The QPT becomes sharp as the current is decreased. Several σ_{xy}-$\cos\theta$ curves for various I cross almost at a single point, exemplifying the QPT between the QAH insulator and the trivial insulator. The crossing point is the QCP of the transition. The crossing point $(\cos\theta, \sigma_{xy}) = (0.38, 0.43e^2/h)$ is almost the same as the QCP in the previous temperature dependence measurement [19]. The parametric plot of $(\sigma_{xy}, \sigma_{xx})$ for various I in the inset of Fig. 3(a) shows a flow as similar to the temperature scaling flow [6,19,25]: $(\sigma_{xx}, \sigma_{xy})$ tends to converge to either $(0, 0)$ or $(e^2/h, 0)$ with decreasing current with an unstable point at around $(0.5e^2/h, 0.5e^2/h)$.

Next, we analyze how the sharpness of the QPT changes with the excitation current. Figure 4(a) shows the I

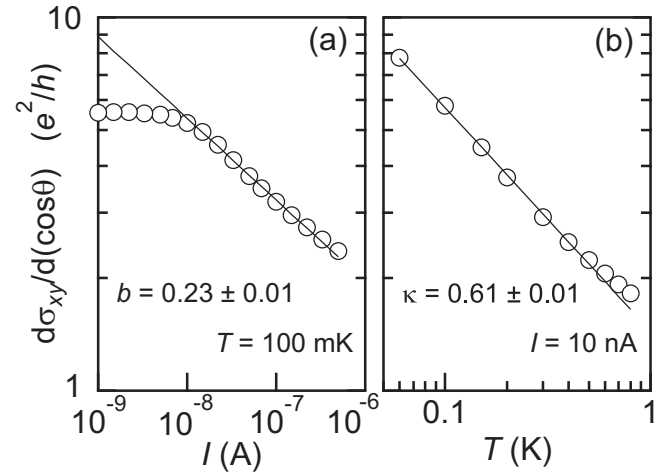

FIG. 4. (a)(b) The slope of the σ_{xy}-$\cos\theta$ curve at the QCP $d\sigma_{xy}/d\cos\theta$ plotted as a function of excitation current (a) and temperature (b). The data in (b) are taken from Ref. [19]. The solid lines are the fitting results to $d\sigma_{xy}/d\cos\theta \propto I^{-b}$ in (a) and $\propto T^{-\kappa}$ in (b), respectively. The measurement temperature was $T = 100$ mK in (a). The excitation current was $I = 10$ nA in (b).

dependence of the slope $d\sigma_{xy}/d\cos\theta(I)$ at the QCP. For comparison, the temperature dependence of $d\sigma_{xy}/d\cos\theta(T)$ taken from the previous study [19] is shown in Fig. 4(b). The slope $d\sigma_{xy}/d\cos\theta(I)$ increases with decreasing I and turns to saturate below $I \sim 10$ nA as shown in Fig. 4(a). Because the current dependence measurement was conducted at $T = 100$ mK, the saturated value shows a good agreement with $d\sigma_{xy}/d\cos\theta$ ($T = 100$ mK) in Fig. 4(b). The saturation in the I dependence indicates that $d\sigma_{xy}/d\cos\theta(I)$ is limited by the thermal excitation in the range $I < 10$ nA while $\sigma_{xy}/d\cos\theta(I)$ is dominated by the excitation current in the range $I \geqslant 10$ nA. For $I \geqslant 10$ nA, the slope follows a power-law current dependence $d\sigma_{xy}/d\cos\theta(I) \sim I^{-b}$ with a current scaling exponent $b = 0.23 \pm 0.01$. Combining b with the temperature scaling exponent $\kappa = 0.61 \pm 0.01$ [19], the critical exponents ν for the localization length and p for the coherence length are separately yielded as $\nu = 2.8 \pm 0.3$ and $p = 3.3 \pm 0.3$.

The value $\nu = 2.8 \pm 0.3$ is reasonably close to the result of the Chalker-Coddington model $\nu = 2.6$ [30,31] and those reported in the QH transitions in InGaAs/InP heterostructure [37,38] but is apparently larger than the exponent 4/3 for the classical percolation in two-dimensional systems [26,27]. This result indicates that the transition between the QAH insulator and the trivial insulator can be modeled by a quantum percolation of a network of chiral edge channels where quantum tunneling at the saddle points dominates the critical behavior [30,40]. According to the earlier studies of the QH transitions [39,44], $l_\phi > \xi$ is an essential condition to obtain the universal critical exponent. A rather short localization length due to strong disorder in the surface state of the magnetic topological insulators [43,45] probably assists this condition to be satisfied. Note that there is no magnetic multidomain structure at the QCP in the present experiment due to the externally applied magnetic field. Therefore, the BKT-type phase transition discussed in Ref. [41] is not likely to occur.

The value $p = 3.3 \pm 0.3$ is considerably large compared to $p \sim 2$ reported in the earlier studies of QH transitions in the InP/InGaAs heterostructures [37,38]. A recent study [39] of the QH transitions in GaAs/AlGaAs heterostructures reports a large variation of p from 0.5 to 3.9 with decreasing mobility. The large values of $p \sim 3$ have been also reported in a GaAs/AlGaAs multi-quantum-well structure [46] and a copper film [47] where the electron-phonon interaction dominates the inelastic scattering time. Our result $p = 3.3 \pm 0.3$ seems to be consistent with these cases of strong electron-phonon coupling and low mobility. In MBE-grown thin films of nonmagnetic $(Bi,Sb)_2Te_3$ thin films, the p value is reported as $0.5 < p < 1$ from the antiweak localization analysis of magnetoconductivity [48]. This result implies that incorporation of the magnetic elements causes the enhancement of p. Besides the phonon scatterings, the effect of magnon scatterings [49] should be taken into consideration as a decoherence source of electrons.

To summarize, the magnetization rotation driven QPT between the QAH insulator and the hybridization-induced trivial insulator is studied as a function of excitation current. The sharpness of the QPT $d\sigma_{xy}/d\cos\theta$ is found to follow a power-law current dependence. Combined with the result of the temperature scaling, the critical exponents for the localization length ν and for the coherence length p are evaluated experimentally. The obtained value of ν is consistent with the results of the Chalker-Coddington model, pointing out that the QAH insulator to trivial insulator transition can be described by a quantum percolation of chiral edge channels.

We acknowledge valuable discussions with Akira Furusaki, Naoto Nagaosa, Kenji Yasuda, and Yayu Wang. This study was supported by MEXT/JSPS KAKENHI Grants No. JP15H0583, No. JP15H05867, No. JP17J03179, No. JP18H04229, No. JP18H01155, and JST CREST Grant No. JPMJCR16F1, Japan.

[1] M. Z. Hasan and C. L. Kane, Colloquium: Topological insulators, Rev. Mod. Phys. **82**, 3045 (2010).
[2] X.-L. Qi and S.-C. Zhang, Topological insulators and superconductors, Rev. Mod. Phys. **83**, 1057 (2011).
[3] B. Yang and C. Felser, Topological materials: Weyl semimetals, Annu. Rev. Condens. Matter Phys. **8**, 337 (2017).
[4] R. Yu, W. Zhang, H.-J. Zhang, S.-C. Zhang, X. Dai, and Z. Fang, Quantized anomalous Hall effect in magnetic topological insulators, Science **329**, 61 (2010).
[5] C.-Z. Chang, J. Zhang, X. Feng, J. Shen, Z. Zhang, M. Guo, K. Li, Y. Ou, P. Wei, L.-L. Wang, Z.-Q. Ji, Y. Feng, S. Ji, X. Chen, J. Jia, X. Dai, Z. Fang, S.-C. Zhang, K. He, Y. Wang, L. Lu, X.-C. Ma, Q.-K. Xue, Experimental observation of the quantum anomalous Hall effect in a magnetic topological insulator, Science **340**, 167 (2013).
[6] J. G. Checkelsky, R. Yoshimi, A. Tsukazaki, K. S. Takahashi, Y. Kozuka, J. Falson, M. Kawasaki, and Y. Tokura, Trajectory of anomalous Hall effect toward the quantized state in a ferromagnetic topological insulator, Nat. Phys. **10**, 731 (2014).
[7] X. Kou, S.-T. Guo, Y. Fan, L. Pan, M. Lang, Y. Jiang, Q. Shao, T. Nie, K. Murata, J. Tang, Y. Wang, L. He, T.-K. Lee, W.-L. Lee, and K. L. Wang, Scale-Invariant Quantum Anomalous Hall Effect in Magnetic Topological Insulators Beyond the Two-Dimensional Limit, Phys. Rev. Lett. **113**, 137201 (2014).
[8] C.-Z. Chang, W. Zhao, D. Y. Kim, H. Zhang, B. A. Assaf, D. Heiman, S.-C. Zhang, C. Liu, M. H. W. Chan, and J. S. Moodera, High-precision realization of robust quantum anomalous Hall state in a hard ferromagnetic topological insulator, Nat. Mater. **14**, 473 (2015).
[9] M. Mogi, R. Yoshimi, A. Tsukazaki, K. Yasuda, Y. Kozuka, K. S. Takahashi, M. Kawasaki, and Y. Tokura, Magnetic modulation doping in topological insulators toward higher-temperature quantum anomalous Hall effect, Appl. Phys. Lett. **107**, 182401 (2015).
[10] S. Grauer, K. M. Fijalkowski, S. Schreyeck, M. Winnerlein, K. Brunner, R. Thomale, C. Gould, and L. W. Molenkamp, Scaling of the Quantum Anomalous Hall Effect as an Indicator of Axion Electrodynamics, Phys. Rev. Lett. **118**, 246801 (2017).

[11] Y. Tokura, K. Yasuda, and A. Tsukazaki, Magnetic topological insulators, Nat. Rev. Phys. **1**, 126 (2019).

[12] C. Liu, Y. Wang, H. Li, Y. Wu, Y. Li, J. Li, K. He, Y. Xu, J. Zhang, and Y. Wang, Robust axion insulator and Chern insulator phases in a two-dimensional antiferromagnetic topological insulator, Nat. Mater. **19**, 522 (2020).

[13] Y. Deng, Y. Yu, M.-Z. Shi, Z. Guo, Z. Xu, J. Wang, X.-H. Chen, and Y. Zhang, Quantum anomalous Hall effect in intrinsic magnetic topological insulator $MnBi_2Te_4$, Science **367**, 895 (2020).

[14] M. Serlin, C. L. Tschirhart, H. Polshyn, Y. Zhang, J. Zhu, K. Watanabe, T. Taniguchi, L. Balents, and A. F. Young, Intrinsic quantized anomalous Hall effect in a moiré heterostructure, Science **367**, 900 (2020).

[15] A. L. Sharpe, E. J. Fox, A. W. Barnard, J. Finney, K. Watanabe, T. Taniguchi, M. A. Kastner, and D. Goldhaber-Gordon, Emergent ferromagnetism near three-quarters filling in twisted bilayer graphene, Science **365**, 605 (2019).

[16] M. Mogi, M. Kawamura, R. Yoshimi, A. Tsukazaki, Y. Kozuka, N. Shirakawa, K. S. Takahashi, M. Kawasaki, and Y. Tokura, A magnetic heterostructure of topological insulators as a candidate for an axion insulator, Nat. Mater. **16**, 516 (2017).

[17] M. Mogi, M. Kawamura, A. Tsukazaki, R. Yoshimi, K. S. Takahashi, M. Kawasaki, and Y. Tokura, Tailoring tricolor structure of magnetic topological insulator for robust axion insulator, Sci. Adv. **3**, eaao1669 (2017).

[18] Y. Zhang, K. He, C.-Z. Chang, C.-L. Song, L.-L. Wang, X. Chen, J.-F. Jia, Z. Fang, X. Dai, W.-Y Shan, S.-Q. Shen, Q. Niu, X.-L. Qi, S.-C. Zhang, X.-C. Ma, and Q.-K. Xue, Crossover of the three-dimensional topological insulator Bi_2Se_3 to the two-dimensional limit, Nat. Phys. **6**, 584 (2010).

[19] M. Kawamura, M. Mogi, R. Yoshimi, A. Tsukazaki, Y. Kozuka, K. S. Takahashi, M. Kawasaki, and Y. Tokura, Topological quantum phase transition in magnetic topological insulator upon magnetization rotation, Phys. Rev. B **98**, 140404(R) (2018).

[20] X. Kou, L. Pan, J. Wang, Y. Fan, E. S. Choi, W.-L. Lee, T. Nie, K. Murata, Q. Shao, S.-C. Zhang, and K.-L. Wang, Metal-to-insulator switching in quantum anomalous Hall states, Nat. Commun. **6**, 8474 (2015).

[21] C.-Z. Chang, W. Zhao, J. Li, J. K. Jain, C. Liu, J. S. Moodera, and M. H. W. Chan, Observation of the Quantum Anomalous Hall Insulator to Anderson Insulator Quantum Phase Transition and Its Scaling Behavior, Phys. Rev. Lett. **117**, 126802 (2016).

[22] Y. Feng, X. Feng, Y. Ou, J. Wang, C. Liu, L. Zhang, D. Zhao, G. Jiang, S.-C. Zhang, Ke He, X. Ma, Q.-K. Xue, and Y. Wang, Observation of the Zero Hall Plateau in a Quantum Anomalous Hall Insulator, Phys. Rev. Lett. **115**, 126801 (2015).

[23] D. J. Thouless, M. Kohmoto, M. P. Nightingale, and M. den Nijs, Quantized Hall Conductance in a Two-Dimensional Periodic Potential, Phys. Rev. Lett. **49**, 405 (1982).

[24] H. Aoki and T. Ando, Critical Localization in Two-Dimensional Landau Quantization, Phys. Rev. Lett. **54**, 831 (1985).

[25] A. M. M. Pruisken, Universal Singularities in the Integral Quantum Hall Effect, Phys. Rev. Lett. **61**, 1297 (1988).

[26] S. A. Trugman, Localization, percolation, and the quantum Hall effect, Phys. Rev. B **27**, 7539 (1983).

[27] D.-H. Lee, Z. Wang, and S. Kivelson, Quantum Percolation and Plateau Transitions in the Quantum Hall Effect, Phys. Rev. Lett. **70**, 4130 (1993).

[28] B. Huckestein, Scaling theory of the integer quantum Hall effect, Rev. Mod. Phys. **67**, 357 (1995).

[29] S. L. Sondhi, S. M. Girvin, J. P. Carini, and D. Shahar, Continuous quantum phase transitions, Rev. Mod. Phys. **69**, 315 (1997).

[30] J. T. Chalker and P. D. Coddington, Percolation, quantum tunneling and the integer Hall effect, J. Phys. C: Solid State Phys. **21**, 2665 (1988).

[31] K. Slevin and T. Ohtsuki, Critical exponent for the quantum Hall transition, Phys. Rev. B **80**, 041304(R) (2009).

[32] H. P. Wei, D. C. Tsui, M. A. Paalanen, and A. M. M. Pruisken, Experiments on Delocalization and University in the Integral Quantum Hall Effect, Phys. Rev. Lett. **61**, 1294 (1988).

[33] S. Koch, R. J. Haug, K. V. Klitzing, and K. Ploog, Size-Dependent Analysis of the Metal-Insulator Transition in the Integral Quantum Hall Effect, Phys. Rev. Lett. **67**, 883 (1991).

[34] M. Hilke, D. Shahar, S. H. Song, D. C. Tsui, Y. H. Xie, and D. Monroe, Experimental evidence for a two-dimensional quantized Hall insulator, Nature (London) **395**, 675 (1998).

[35] W. Li, G. A. Csáthy, D. C. Tsui, L. N. Pfeiffer, and K. W. West, Scaling and Universality of Integer Quantum Hall Plateau-to-Plateau Transitions, Phys. Rev. Lett. **94**, 206807 (2005).

[36] D. G. Polyakov and B. I. Shklovskii, Conductivity-peak broadening in the quantum Hall regime, Phys. Rev. B **48**, 11167 (1993).

[37] H. P. Wei, L. W. Engel, and D. C. Tsui, Current scaling in the integer quantum Hall effect, Phys. Rev. B **50**, 14609 (1994).

[38] W. Pan, D. Shahar, D. C. Tsui, H. P. Wei, and M. Razeghi, Quantum Hall liquid-to-insulator transition in $In_{1-x}Ga_xAs/InP$ heterostructures, Phys. Rev. B **55**, 15431 (1997).

[39] N. A. Dodoo-Amoo, K. Saeed, D. Mistry, S. P. Khanna, L. Li, E. H. Linfield, A. G. Davies, and J. E. Cunningham, Non-universality of scaling exponents in quantum Hall transitions, J. Phys.: Condens. Matter **26**, 475801 (2014).

[40] J. Wang, B. Lian, and S.-C. Zhang, Universal scaling of the quantum anomalous Hall plateau transition, Phys. Rev. B **89**, 085106 (2014).

[41] C.-Z. Chen, H. Liu, and X. C. Xie, Effects of Random Domains on the Zero Hall Plateau in the Quantum Anomalous Hall Effect, Phys. Rev. Lett. **122**, 026601 (2019).

[42] J. Wang, B. Lian, and S.-C. Zhang, Quantum anomalous Hall effect in magnetic topological insulators, Phys. Scr., T **164**, 014003 (2015).

[43] M. Kawamura, R. Yoshimi, A. Tsukazaki, K. S. Takahashi, M. Kawasaki, and Y. Tokura, Current-Driven Instability of the Quantum Anomalous Hall Effect in Ferromagnetic Topological Insulators, Phys. Rev. Lett. **119**, 016803 (2017).

[44] W. Li, J. S. Xia, C. Vicente, N. S. Sullivan, W. Pan, D. C. Tsui, L. N. Pfeiffer, and K. W. West, Crossover from the nonuniversal scaling regime to the universal scaling regime in quantum Hall plateau transitions, Phys. Rev. B **81**, 033305 (2010).

[45] I. Lee, C. K. Kim, J. Lee, S. J. L. Billinge, R. Zhong, J. A. Schneeloch, T. Liu, T. Valla, J. M. Tranquada, G. Gu, and J. C. Séamus Davis, Imaging Dirac-mass disorder from magnetic dopant atoms in the ferromagnetic topological insulator $Cr_x(Bi_{0.1}Sb_{0.9})_{2-x}Te_3$, Proc. Natl. Acad. Sci. USA **112**, 1316 (2015).

[46] A. K. M. Wennberg, S. N. Ytterboe, C. M. Gould, H. M. Bozler, J. Klem, and H. Morkoç, Electron heating in a multiple-quantum-well structure below 1 K, Phys. Rev. B **34**, 4409 (1986).

[47] M. L. Roukes, M. R. Freeman, R. S. Germain, R. C. Richardson, and M. B. Ketchen, Hot Electrons and Energy Transport in Metals at Millikelvin Temperatures, Phys. Rev. Lett. **55**, 422 (1985).

[48] J. Liao, Y. Ou, H. Liu, K. He, X. Ma, Q.-K. Xue, and Y. Li, Enhanced electron dephasing in three-dimensional topological insulators, Nat. Commun. **8**, 16071 (2017).

[49] K. Yasuda, A. Tsukazaki, R. Yoshimi, K. S. Takahashi, M. Kawasaki, and Y. Tokura, Large Unidirectional Magnetoresistance in a Magnetic Topological Insulator, Phys. Rev. Lett. **117**, 127202 (2016).